Optimising the synthesis of shaped beam antenna patterns

H.J. Orchard, M.Sc., C.Eng., F.I.E.E., Fel.I.E.E.E., Prof. R.S. Elliott, Ph.D.,
Fel.I.E.E.E., and G.J. Stern, M.Sc., Sen.Mem.I.E.E.E.

Indexing terms: Antennas, Mathematical techniques

Abstract: A technique is introduced which uses the conventional polynomial representation of the antenna pattern produced by an equispaced linear array. Certain roots are displaced from the unit circle radially, to fill a portion of the pattern, which before this displayed lobes interspersed by deep nulls. The angular and radial positions of all the roots are simultaneously adjusted so that the amplitude of each ripple in the shaped region and the height of each sidelobe in the nonshaped region are individually controlled. Applications to a $\csc^2 \theta \times \cos \theta$ pattern and to a flat-topped beam are presented. Experimental validation is also offered.

1 Introduction

Recently a pattern synthesis technique was described which yields the excitation of an equispaced linear array that will produce a shaped-beam pattern with arbitrary sidelobe topography in the nonshaped region [1]. The technique relied on an earlier procedure for generating a suitable starting pattern, which used a polynomial representation of the pattern, with all roots on the Schelkunoff unit circle [2], the positions of these roots being iteratively adjusted to yield a sum pattern with the height of each sidelobe independently specified [3].

The sidelobe heights in the starting pattern were adjusted so that, in the region to be shaped (Region I), they coincided with the desired shaping contour C. Elsewhere (Region II) they were adjusted to agree with the specified sidelobe topography. This starting pattern was then perturbed by moving certain roots radially off the unit circle to cause null filling in Region I. Trial and error adjustment of the starting pattern and of the radial root displacements resulted in a satisfactory approximation to the desired shaped-beam pattern.

This recent pattern synthesis technique provided, for the first time, a means of obtaining arbitrary sidelobe topography in Region II. However, it suffers from several shortcomings. Foremost is the trial and error feature, which requires the generation of a second starting pattern to get the main beam height set properly with respect to the family of sidelobes, and which requires adjustment of the radial root displacements in order to balance the ripple amplitudes in the shaped region. Additionally, the technique does not provide for independent control of the amplitude of each ripple cycle.

The procedure to be described in this paper overcomes these shortcomings by permitting, at the outset, angular as well as radial displacements of the roots in Region I, and angular displacements of the roots in Region II. An additional control parameter is introduced to prevent the main beam height from floating with respect to the sidelobes. Computational efficiency is improved by eliminating the need for a starting pattern whose lobes have the desired shaping contour as an envelope in Region I.

2 Analysis

The far-field array factor of an equispaced linear array can be expressed in the form

$$F = \sum_{n=0}^{N} I_n e^{jnkd \cos \theta} \tag{1}$$

in which I_n is the excitation coefficient of the nth radiating element, d is the interelement spacing, and θ is measured from endfire. In eqn. 1, the element factor has been suppressed. With the usual substitutions

$$\psi = kd \cos \theta \quad \text{and} \quad w = e^{j\psi} \tag{2}$$

the pattern function becomes

$$F = \sum_{n=0}^{N} I_n w^n = I_N \sum_{n=1}^{N} (w - w_n) \tag{3}$$

Writing $w_n = \exp(a_n + jb_n)$, where a_n and b_n are both real, we get

$$|F|^2 = |I_N|^2 \prod_{n=1}^{N} [1 - 2e^{a_n} \cos(\psi - b_n) + e^{2a_n}] \tag{4}$$

With the Nth root anchored at $w_N = -1$, i.e. with $a_N = 0$ and $b_N = \pi$, the power pattern expressed in decibels can be written as

$$G = \sum_{n=1}^{N-1} 10 \log_{10} [1 - 2e^{a_n} \cos(\psi - b_n) + e^{2a_n}]$$
$$+ 10 \log_{10} [2(1 + \cos \psi)] + C_1 \tag{5}$$

The added constant C_1 allows the value of G at the peak of the main beam to be set to any convenient reference value, normally 0 dB.

With no loss of generality we can arrange Region I (the shaped-beam region) to lie immediately adjacent to $\psi = \pi$, and so the behaviour of G as a function of ψ is as shown in Fig. 1. Let the number of roots to be positioned in Region I be N_1 and in Region II be N_2, so that the total number of w_n, including the one fixed at $w = -1$, is $N_1 + N_2$
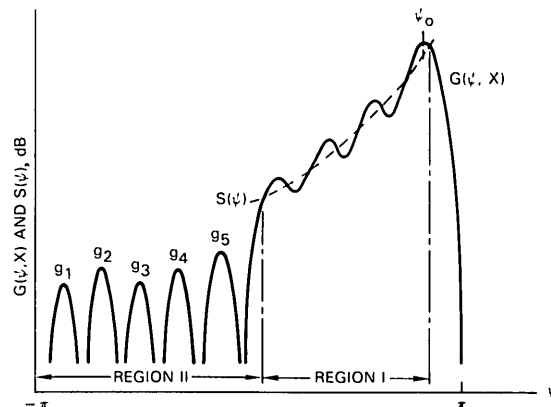

Fig. 1 Identification of shaped region, sidelobe region, desired contour and sidelobe topography, and approximating function

$+ 1 = N$. The N_1 roots in Region I are arranged to lie outside the unit circle, so that $a_n > 0$, and both the a_n and b_n are adjustable, whereas the N_2 zeros in Region II are constrained to lie on the unit circle, making $a_n = 0$ and leaving only the b_n adjustable. There is one more parameter available for use in the design, namely the added constant C_1 in eqn. 5, giving a total of $2N_1 + N_2 + 1 = N_3$. These N_3 parameters are assumed assembled, in any convenient order, as the components of the column vector x. G is thus a function of both ψ and the vector x, which we shall indicate, when necessary, by writing it as $G(\psi, x)$. Note that in Fig. 1, $N_1 = 3$, $N_2 = 5$, and hence $N_3 = 12$.

A shaping function $S(\psi)$, in decibels, which represents the ideal behaviour of G over Region I, must also be prescribed. This is indicated by the dotted line marked S in Fig. 1. In a general-purpose design program it proves convenient to specify $S(\psi)$ by means of an approximating polynomial rather than by the exact, and possibly rather complicated, ideal function. Any function can then be accommodated by supplying the program with the appropriate numerical values of the coefficients, and the program can find easily, in a standard fashion, the values of $S(\psi)$ and its various derivatives that are needed. This is described in Appendix 9.1.

In practice, over Region I, G can only approximate S, and will do so most efficiently if it oscillates around S the maximum possible number of times, so that the deviation behaves as in Fig. 2. The values at the maxima and
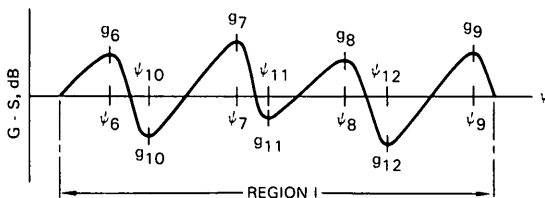

Fig. 2 *Ripple peaks and troughs relative to the desired contour*

minima of $G - S$ can all be specified arbitrarily to obtain the best practical compromise between ripple size and complexity of aperture excitations. As a special case they can all be made equal. To achieve this best oscillatory approximation to $S(\psi)$, and also to fix the peak of the main beam at 0 dB, the absolute level of the shaping curve must be allowed to float up or down slightly. In other words, $S(\psi)$ must also contain an added constant C_2 which is exactly analogous to the constant C_1 in eqn. 5. There is thus a total of $N_3 + 1$ parameters altogether which must be chosen in the design, although the choice of C_2 can be made separately from the other N_3 which are handled through the vector x in the main optimisation loop.

Finally, the performance of $G(\psi, x)$ must be specified by means of the desired values of G at the N_2 maxima in Region II, and at the $N_1 + 1$ maxima and N_1 minima of the function $G - S$ in Region I. These N_3 values, denoted by g_i ($i = 1, 2, \ldots, N_3$), are all assumed to occur when the value of G at the peak of the main beam is adjusted to 0 dB. The g_i are assumed assembled, again in any convenient order, as the components of a column vector g.

The design of $G(\psi, x)$ to meet this specification can be handled by using a variant of the Remez algorithm [4]. An initial requirement is some set of approximate values for the components of the parameter vector x which cause G in Region II and $G - S$ in Region I to have the correct number of maxima and minima; here this proves to be quite simple. Then the ψ values of these maxima and minima are found. Let these values be denoted by $\psi_i (i = 1, 2, \ldots, N_3)$, arranged so that ψ_i is the ψ where g_i is the desired value of G or $G - S$.

For each of these N_3 values of the ψ_i compute the value of $G(\psi_i, x)$ if ψ_i is in Region II, or of $G(\psi_i, x) - S(\psi_i)$ if ψ_i is in Region I, and then assemble these values as the components of a column vector $\hat{g}$, with the same ordering as for the components of g. $\hat{g}$ is thus the approximation at the present stage in the design to the desired vector g. Next, find the Jacobian matrix A whose components $a_{i,j}$ are defined by

$$a_{i,j} = \frac{\partial G(\psi_i, x)}{\partial x_j} \quad (i, j = 1, 2, \ldots, N_3) \tag{6}$$

As $S(\psi)$ is independent of x, the jth column of A is effectively $\partial \hat{g}/\partial x_j$.

Now seek a correction Δx to the approximate vector x which will cause $\hat{g}$ to become a better approximation to g. Using the linear part of the Taylor's series for $\hat{g}$ one obtains the following linear equation for Δx:

$$\hat{g} + A \, \Delta x = g \tag{7}$$

The solution of eqn. 7 for Δx, $x + \Delta x$ can be taken as a better approximate vector. This completes the basic iteration step which is then repeated until the error between $\hat{g}$ and g is small enough for the purpose of the design.

This iteration will cause the values of G over the shaped region to settle at a level which will allow it to approximate $S(\psi)$ in the required way. All N_3 parameters, including C_1, are needed to achieve this. As a result, it is not also possible to control the value of G at the peak of the main beam, which will usually end up close to, but not exactly at, 0 dB. The constant C_2 associated with $S(\psi)$ is used to correct for this small error.

At the beginning of each iteration locate the ψ value of the peak of the main beam, say ψ_0, and then compute $G(\psi_0, x)$. If this value is, e.g. -1 dB, then the curve described by $S(\psi)$ needs to be raised by 1 dB in order to bring up the height of the main beam by 1 dB. This is achieved by decreasing C_2 by $G(\psi_0, x)$.

If C_2 is corrected in this way during each iteration, it rapidly settles down to a value that will cause $G(\psi_0, x)$ to go to zero without much effect on the rate of convergence of the iteration. C_2 could be included as one of the parameters in the vector x and its value found, along with all the others, in the main iteration; but this complicates the program slightly and increases the time of each iteration. For some designs, e.g. a pattern with a flat-topped beam, C_2 is not needed at all, and by using the proposed method it is easier to arrange to ignore it.

The starting values for the parameters a_n and b_n are not especially critical as long as they lead to well defined maxima for G in Region II and maxima and minima for $G - S$ in Region I. A simple choice, which proves quite satisfactory, is to place the ψ_n at equal angular intervals by using

$$\psi_n = \left(\frac{2n}{N + 1} - 1 \right) \pi \quad (n = 1, 2, \ldots, N - 1) \tag{8}$$

With this numbering, the first N_2 roots will lie in Region II, and hence on the unit circle, and so

$$a_n = 0 \quad (n = 1, 2, \ldots, N_2) \tag{9}$$

The next N_1 roots will be in Region I and must be located slightly outside† the unit circle; it appears to be sufficient to set

---

† Choosing these roots to lie outside the unit circle, rather than inside, is done merely for uniformity in the design and to make the a_n positive. Reversing the sign of any a_n leaves the shape of the power pattern unchanged but moves the corresponding zero to the reciprocal point on the same radius. There are thus 2^{N_1} different patterns of roots, and hence sets of excitations I_n, for the designer to choose from, all giving the same pattern. This can be advantageous when the ability for physical realisation for an actual array is in question due to mutual coupling.

$$a_n = 0.01 \quad (n = N_2 + 1, N_2 + 2, \ldots, N - 1) \qquad (10)$$

For the example illustrated in Figs. 1 and 2 these starting w_n values would be as shown in Fig. 3. The initial value for C_1 is not important and can be made zero.
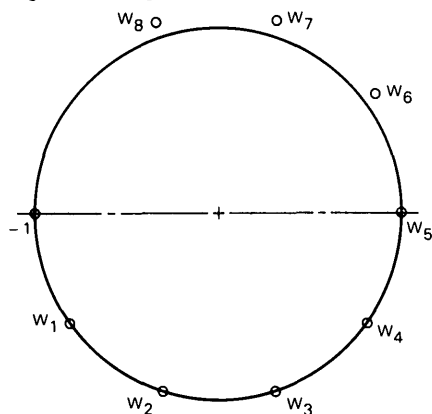

Fig. 3 *The complex w-plane and identification of roots on and off the Schelkunoff unit circle*

The maxima of G in Region II are the zeros of the derivative of G; and the maxima and minima of $G - S$ in Region I are the zeros of the derivative of $G - S$, all with respect to ψ. The fastest way of finding the ψ_i is to use the Newton method to find the zeros of the derivative of the function concerned. The first and second derivatives of G and S both need to be found, and the formulas for these, and a brief discussion of the Newton method, are given in Appendix 9.2.

During each iteration the existence of all these maxima and minima, in the correct order, is relied upon for this Newton process to converge, and hence for the remaining steps to be possible. One potential danger is that the correction vector Δx found from eqn. 7 might change the a_n parameter values enough to destroy the oscillatory behaviour of $G - S$ in Region I, particularly if the desired ripple size is small.

However, all the evidence obtained from several designs is that Δx always gives corrections to the a_n that are smaller than are needed, so that the a_n move monotonically towards their final values. Hence if an oscillatory behaviour in Region I has bigger ripples than needed, then this oscillatory behaviour will be preserved after each correction. A proof that this must necessarily happen would be reassuring, and may well be possible, but has not yet been formulated.

Generally, the iteration seems to be very stable and converges rapidly from the starting point described. The convergence can be checked by monitoring the component of $\hat{g} - g$ with the largest absolute value. Typically about ten iterations are needed to reduce this quantity below 0.01 dB.

3 Application to a $\operatorname{cosec}^2 \theta \times \cos \theta$ pattern

A filled-in pattern of wide applicability has a $\operatorname{cosec}^2 \theta \times \cos \theta$ shape in Region I, since this gives round-trip signals that are θ independent, a desirable feature for ground-mapping radars and aircraft beacons. As an example of this type of pattern, consider a sixteen element equispaced linear array, with $d = \lambda/2$, to be excited to approximate $\operatorname{cosec}^2 (\theta - \pi/2) \times \cos (\theta - \pi/2)$ in $\theta_0 \leqslant \theta \leqslant \theta_1$, with $\theta_0 = 100°$ the main beam position and $\theta_1 = 140°$ the terminus of the filled-in region. The first four sidelobes on the other side of the main beam are to be at -30 dB; all other sidelobes should be at -20 dB.[†]

[†] This reproduces the example used in Reference 1, but with improvements.

When the synthesis procedure just described is applied to this problem it is found that four roots must be displaced from the unit circle in order to fill in the pattern in Region I. When all ripple peaks and troughs are specified to be ± 1.5 dB from the desired contour, the pattern of Fig. 4a results. A ± 1 dB specification yields Fig. 4b, a ± 0.5 dB requirement gives Fig. 4c, and a goal of ± 0.1 dB produces Fig. 4d.

These four patterns demonstrate, by example, that it is indeed possible to control the ripple amplitude in Region I and also the sidelobe topography in Region II. A careful study of enlargements of these patterns reveals a disadvantage of diminishing the ripple amplitude. The extent of
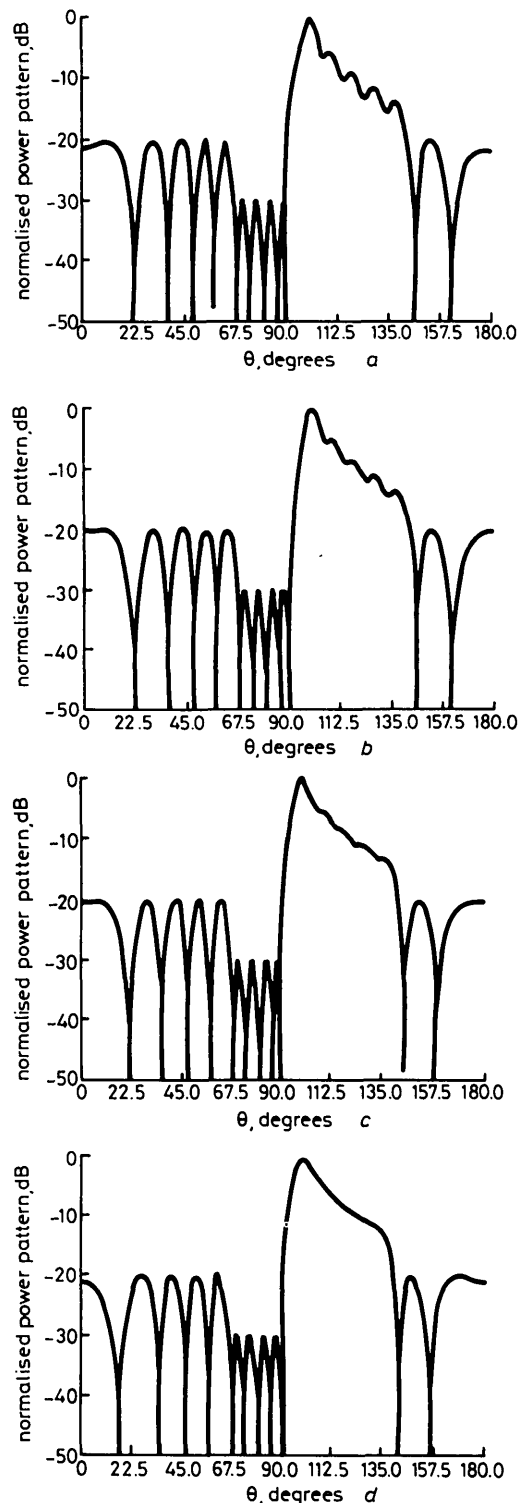

Fig. 4 *$\operatorname{cosec}^2 \theta \times \cos \theta$ patterns produced by a 16 element linear array, $d = \lambda/2$. Ripple requirement:*

a ± 1.5 dB	*c* ± 0.5 dB
b ± 1.0 dB	*d* ± 0.1 dB

Region I monotonically decreases from 41° with a ±1.5 dB ripple to 34° with a ±0.1 dB ripple.†

The disadvantage arises from the complexity of the array excitation. Table 1 lists the most favourable set of currents that will produce the pattern of Fig. 4d. The sense in which 'most favourable' is being used can be described as follows: Since each of the N_1 roots which lie off the unit

Table 1: Current distribution for most favourable of 16 excitations that will produce Figs. 4a, 4d and 6

n	I_n for Fig. 4a		I_n for Fig. 4d		I_n for Fig. 6	
1	0.77	177.1°	1.68	−99.9°	0.99	−7.6°
2	0.50	−89.2°	1.69	−3.8°	1.46	23.2°
3	0.38	−76.0°	1.45	64.0°	1.18	78.4°
4	0.56	−88.3°	0.87	−158.3°	1.42	138.7°
5	0.76	−38.1°	1.83	−48.7°	1.12	−138.7°
6	0.63	7.7°	2.74	22.2°	2.26	−73.8°
7	0.56	−5.0°	3.03	70.5°	2.35	−54.8°
8	0.99	19.0°	2.94	105.7°	1.29	−27.3°
9	1.04	66.8°	3.13	142.3°	1.32	−25.7°
10	0.81	94.1°	3.14	−178.0°	2.32	−52.9°
11	1.03	96.9°	2.50	−141.6°	2.38	−76.8°
12	1.47	132.2°	1.86	−110.8°	1.12	−141.3°
13	1.66	−176.8°	1.74	−80.4°	1.42	134.7°
14	1.64	−126.1°	1.39	−46.1°	1.30	76.1°
15	1.17	−76.4°	0.34	16.9°	1.30	13.4°
16	1.00	0.0°	1.00	0.0°	1.00	0.0°

circle can be either inside or outside, there are 2^{N_1} sets of roots that correspond to the same pattern, and thus 2^{N_1} sets of currents. In this example there are thus sixteen independent excitations which will produce Fig. 4a, another sixteen which will yield Fig. 4b, etc. When all sixteen excitations corresponding to Fig. 4a are examined, it is found that the phase distributions are not particularly dissimilar in their variability, but some of the amplitude distributions show considerably more variability than others. Amplitude variability exacerbates the mutual coupling problem, so a rough criterion for physical realisability could be that the set of currents which shows the least amplitude variability should be chosen from among the 16 possibilities.* This has been done in composing Table 1.

From a study of this Table it can be seen that the excitations required to produce the patterns of Figs. 4a and 4d are both reasonable enough to be achieved in practice, but that the maximum/minimum amplitude ratio is only 4.34 for the ±1.5 dB case, whereas it is 9.27 for the ±0.1 dB case. Table 2, which shows current ratios for all four patterns of Fig. 4, strengthens the argument. A reduced ripple amplitude requires an array excitation which is more difficult to achieve.

Table 2: Amplitude ratios for the 16 possible array excitations corresponding to the patterns of Fig. 4

Ripple	Least I_{max}/I_{min}	Greatest I_{max}/I_{min}	Average I_{max}/I_{min}
±1.5 dB	4.34	7.36	5.87
±1.0 dB	3.97	9.76	6.62
±0.5 dB	5.15	51.16	13.39
±0.1 dB	9.27	55.87	20.60

In some applications, suppression of the ripple is of

---

† Thus it would be necessary to move five roots off the unit circle if a ±0.1 dB ripple were specified and $\theta_1 = 140°$ were held firm.

* We are presently making a case study of the actual mutual coupling values in a 16 by 16 slot array for each of these possible excitations to see if there is a correlation to amplitude variability.

decreasing importance as the main beam is departed from. Fig. 5 illustrates how the synthesis procedure can be applied to such situations. In that Figure the ripple amplitude has been allowed to expand linearly from 0.2 dB to 1.0 dB. Easing up on the ripple requirement in this manner results in less demanding array excitations. I_{max}/I_{min} is only 4.44 for the most favourable of the sixteen distributions that will produce Fig. 5.
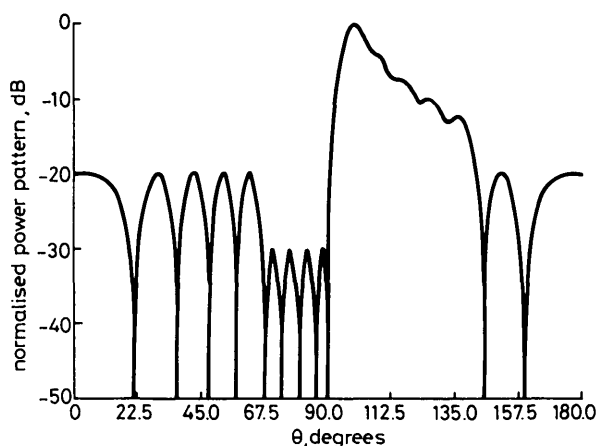

Fig. 5 $cosec^2\ \theta \times \cos\ \theta$ pattern produced by a 16 element linear array, $d = \lambda/2$. Ripple requirement: 0.2 dB at main beam, expanding to 1.0 dB at end of shaped beam

4 Application to a flat-topped beam

Some applications require a pattern that will provide uniform coverage in a certain angular region and a controlled sidelobe level elsewhere. An example of this is shown in Fig. 6. The 16-element array has been adapted to the specification that a flat-topped beam, with a ripple not to exceed ±0.5 dB, should extend over the region $65° \leqslant \theta \leqslant 115°$. The sidelobes on one side are all to be at −30 dB whereas on the other side they should all be at −20 dB.

The most favourable current distribution that will produce this pattern is listed in the last column of Table 1 and is seen to be well within the state of the art.

5 Experimental validation

With ultimate application to a terrain avoidance radar in mind, Rantec undertook to test this pattern synthesis technique by constructing a 2-dimensional slot array consisting of 26 branch line waveguides, each containing six broad wall longitudinal slots. The E-plane pattern was to be within ±2 dB of $cosec^2\ (\theta - 96°) \times \cos\ (\theta - 96°)$ in $96° \leqslant \theta \leqslant 140°$, with θ measured from the zenith. Outside
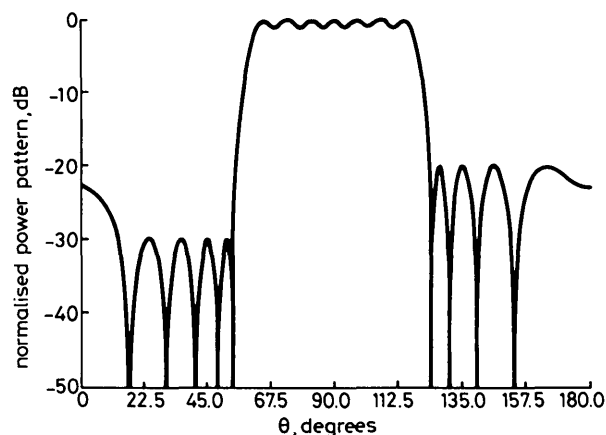

Fig. 6 Flat-topped beam with ±0.5 dB ripple. −30 dB sidelobes, one side. −20 dB sidelobes other side

this range, the side lobes were to fall off as they would in a uniformly excited array. The H-plane excitation was to be uniform and the sum of the normalised active admittances in a branch line was to have the common value 4. The excitations were first found, using the technique described earlier in this paper, with all the radially displaced roots (11 in number) outside the unit circle. Using a slot array design procedure described elsewhere [7], we discovered that some of the mutual coupling values were out of bounds, i.e. the excitations were not physically realisable. A computer search of the 2^{11} possibilities was undertaken and it was found that the 1010th case gave minimum amplitude variability, and also resulted in mutual coupling values that could be compensated. An array was constructed using this excitation and the E-plane pattern at the design frequency (15 GHz) is shown in Fig. 7. It is
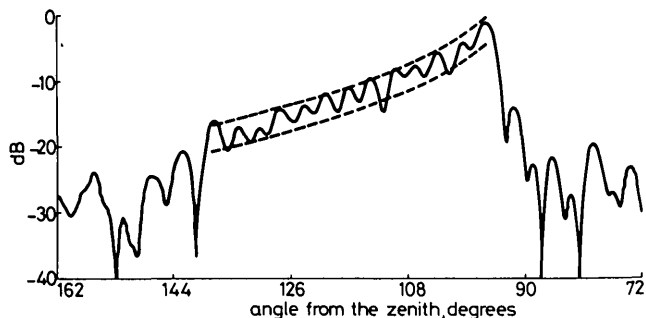

Fig. 7 *Experimental E-plane pattern for 6 by 26 slot array. 15 GHz. $cosec^2$ $(\theta - 96°) \times cos$ $(\theta - 96°)$ in $96° \leqslant \theta \leqslant 140°$. Contours shown at ± 2 dB. (Courtesy of Rantec)*

gratifying to see that most of the shaped region is within the ± 2 dB contours. Probing each branch line, we found that all but two amplitudes were within 1% of design, and all phases were within $\pm 5°$ of design. It can be concluded from this that the tolerances on excitation are reasonable in an extreme practical test, since mutual coupling is severe in the E-plane, which in this case was the plane in which the pattern was to be shaped.

6 Conclusions

A synthesis procedure has been devised which is applicable to the design of equispaced linear arrays that will produce filled-in patterns. The procedure permits individual control of every ripple peak and trough in the shaped region. There are 2^{N_1} possible array excitations, with N_1 the number of roots not lying on the Schelkunoff unit circle. This is an important advantage when the ability for physical realisation in the face of mutual coupling is considered.

The price paid for a reduced ripple is a shrinkage of the shaped region (N_1 fixed) and an increase in complexity of the array excitation.

Applications to $cosec^2$ $\theta \times cos$ θ type pattern and to flat-topped beams have been used to illustrate the procedure.

Extension to planar arrays proceeds directly via the collapsed distribution principle.

7 Acknowledgments

8 References

1 ELLIOTT, R.S., and STERN, G.J.: 'A new technique for shaped beam synthesis of equispaced arrays', to appear in *IEEE Trans. Anennas and Propagation*
2 SHELKUNOFF, S.A.: 'A mathematical theory of linear arrays', *Bell Syst. Tech. J.*, 1943, 22, pp. 80–107
3 ELLIOTT, R.S.: 'Improved pattern synthesis for equispaced linear arrays', *Alta Freq.*, 1982, 51, pp. 296–300
4 REMEZ, E.: 'Sur le calcul effectif des polynomes d'approximation de Tchebychef', *Compt. Rend. Acad. Sci (Paris)*, 1934, 199, pp. 337–340
5 WILKINSON, J.H.: 'The evaluation of the zeros of ill-conditioned polynomials', *Numer. Math.*, 1959, 1, pp. 150–180
6 LANCZOS, C.: Tables of Chebyshev polynomials. US Department of Commerce, National Bureau of Standards Applied Mathematics Series 9, Washington, 1952 (Introduction, pp. XVI–XVIII)
7 ELLIOTT, R.S.: 'An improved design procedure for small slot arrays', *IEEE Trans.*, 1983, AP-31, pp. 48–53

9 Appendix

9.1 Polynomial approximation of the shaping function

The shaping contour for the main beam is intrinsically prescribed in terms of the variable θ in eqn. 1; it will usually be referenced to the specified value of θ at the peak of the main beam, say θ_0, which corresponds to ψ_0, and be required to be approximated over some range $\theta_0 \leqslant \theta \leqslant \theta_1$. Let this shaping contour, expressed in decibels, be $C(\theta)$ with $C(\theta_0) = 0$.

The pattern of zeros in the w-plane produced by the present design has w_N anchored arbitrarily at $w = -1$, so it is necessary to rotate the pattern by some angle ψ_r until ψ_0 and θ_0 are related by eqn. 2. The ψ variable used in the design is thus related to θ by

$$\psi - \psi_r = kd \cos \theta \qquad (11)$$

and

$$\psi_0 - \psi_r = kd \cos \theta_0$$

and hence

$$\psi - \psi_0 = kd (\cos \theta - \cos \theta_0) \qquad (12)$$

As the shaping function $S(\psi)$ and its derivatives have to be evaluated many times in each iteration, less computing will be needed if the polynomial approximation is arranged to be one that is effectively in ψ rather than θ. However, as ψ_0 (and hence ψ_r) changes during the iteration, and as the final value cannot be known before completing the design, the polynomial can only be in a variable that is linearly related to ψ. Use is made of this to choose the polynomial variable, which is denoted by y, so that the range of approximation is $-1 \leqslant y \leqslant 1$ to give a polynomial having the least ill conditioning with respect to its coefficients [5].

If ψ_1 is the value corresponding to θ_1 from eqn. 12, then the linear relation between y and ψ which effectively maps $\theta_0 \leqslant \theta \leqslant \theta_1$ into $-1 \leqslant y \leqslant 1$ is

$$y = \frac{\psi - \psi_0}{\psi_1 - \psi_0} + \frac{\psi - \psi_1}{\psi_1 - \psi_0}$$

$$= \frac{2}{\psi_1 - \psi_0} (\psi - \psi_0) - 1$$

$$= t_1(\psi - \psi_0) - 1 \qquad (13)$$

where

$$t_1 = \frac{2}{\psi_1 - \psi_0} = \frac{2}{kd (\cos \theta_1 - \cos \theta_0)} \qquad (14)$$

The coefficient t_1 in eqn. 13 does not change during the

design and can be computed before the iteration starts. ψ_0 is updated during each iteration, and the generation of the y corresponding to any ψ involves only one multiplication and two subtractions.

If one substitutes kd ($\cos\theta - \cos\theta_0$) for $\psi - \psi_0$ in eqn. 13, θ can be solved in terms of y to obtain

$$\theta = \cos^{-1}(d_1 y + d_0) \qquad (15)$$

where

$$d_1 = \frac{\cos\theta_1 - \cos\theta_0}{2}$$

and

$$d_0 = \frac{\cos\theta_1 + \cos\theta_0}{2}$$

With the change of variable in eqn. 15 $C(\theta)$ becomes $\hat{C}(y)$, and a polynomial $P(y)$ is sought which approximates $\hat{C}(y)$ over $-1 \leqslant y \leqslant 1$. This is easily found by first expressing $\hat{C}(y)$ as a Chebyshev polynomial series as far as the nth term [6].

$$\hat{C}(y) = \tfrac{1}{2}c_0 T_0(y) + c_1 T_1(y) + \cdots + c_{n-1} T_{n-1}(y) + \tfrac{1}{2}c_n T_n(y) \qquad (16)$$

where the coefficients c_k are found from

$$c_k = \frac{2}{n} \sum_{m=0}^{n}{}'' \hat{C}\left(\cos\frac{m\pi}{n}\right) \times \cos\left(\frac{mk\pi}{n}\right) \qquad (17)$$

in which $\sum''$ indicates that the first and last terms in the summation are to be halved.

The value of n is chosen to be large enough so that $|c_n|$ is much smaller than the error which can be tolerated between $P(y)$ and $\hat{C}(y)$. If $\hat{C}(y)$ is a smooth, continuous function, the coefficients c_k will decay rapidly in magnitude and the maximum error in the polynomial formed by truncating the series in eqn. 16 after c_j will be roughly $|c_{j+1}|$. $P(y)$ is then taken as a suitably truncated version of eqn. 16 and its polynomial coefficients found from the c_k that are retained.

To illustrate this, consider the shaping contour

$$C(\theta) = 10\,\log_{10}\left\{\frac{\sin(\theta_0 - \pi/2)\tan(\theta_0 - \pi/2)}{\sin(\theta - \pi/2)\tan(\theta - \pi/2)}\right\}$$

With $\theta_0 = 100°$, $\theta_1 = 140°$ and $n = 20$, the coefficients c_k given in Table 3 to four decimal places are obtained; to this accuracy they are zero after c_{10}. The coefficients p_k of the polynomial

$$P(y) = p_0 y^6 + p_1 y^5 + \cdots + p_5 y + p_6 \qquad (18)$$

formed by truncating after c_6 are also given in Table 3.

Table 3: Coefficients of c_k and p_k

k	c_k	p_k
0	−16.6128	0.1663
1	−7.0497	−0.3498
2	0.8690	0.2252
3	−0.2986	−0.7571
4	0.0593	1.3569
5	−0.0219	−6.2633
6	0.0052	−9.1213
7	−0.0019	
8	0.0005	
9	−0.0002	
10	0.0001	

9.2 Derivatives of $G(\psi, x)$ and $S(\psi)$

The fastest way to find the maxima and minima of

$G(\psi, x) - S(\psi)$ in Region I and the maxima of $G(\psi, x)$ in Region II is to use the Newton process to locate the zeros of the derivatives of the functions concerned. This requires the computation of the first and second derivatives of $G(\psi, x)$ and $S(\psi)$ with respect to ψ. For $G(\psi, x)$ the formulas are

$$\frac{dG}{d\psi} = M \sum_{n=1}^{N-1} \frac{e^{a_n}\sin(\psi - b_n)}{D_n} - \frac{M\sin\psi}{2(1 + \cos\psi)} \qquad (19)$$

$$\frac{d^2G}{d\psi^2} = M \sum_{N=1}^{N-1} \frac{e^{a_n}[(1 + e^{2a_n})\cos(\psi - b_n) - 2e^{a_n}]}{D_n^2}$$

$$- \frac{M}{2(1 + \cos\psi)} \qquad (20)$$

where $M = 20/\ln 10$ and $D_n = 1 - 2e^{a_n}\cos(\psi - b_n) + e^{2a_n}$.

For $S(\psi)$, the corresponding calculation must be carried out on the approximating polynomial $P(y)$. If the coefficients of $P(y)$, as defined in eqn. 18, are assumed stored in a computer in a subscripted variable with p_k in $P(k)$, and if the degree of $P(y)$ is L, then the following simple BASIC program will generate, simultaneously, $P(y)$, $P'(y)$ and $P''(y)/2!$ in P0, P1 and P2, respectively:

```
P0 = P(0)
P1 = 0
P2 = 0
FOR I = 1 TO L
P2 = P2*Y + P1
P1 = P1*Y + P0
P0 = P0*Y + P(I)
NEXT I
```

From eqn. 13 we find the final formulas for the derivatives of $S(\psi)$ as

$$\frac{dS}{d\psi} = \frac{dP}{dy} \times \frac{dy}{d\psi} = t_1 \frac{dP}{dy} \qquad (21)$$

$$\frac{d^2S}{d\psi^2} = \frac{d^2P}{dy^2}\left(\frac{dy}{d\psi}\right)^2 = t_1^2 \frac{d^2P}{dy^2} \qquad (22)$$

The starting value for the Newton iteration for each maximum in Regions I and II can be taken as the arithmetic mean of the b_n values of the two zeros between which it lies, while for each minimum in Region I the starting value can be taken as the b_n value of the zero to which it is immediately adjacent. These starting values are correct to a few percent and the iteration usually converges to an accuracy of six decimal places within two or three cycles. There is no point in finding the maxima or minima more accurately than this, and as the convergence is quadratic at that stage a convenient criterion for stopping the iteration is when the correction has an absolute value equal to or less than 10^{-4}.

The same technique can be used for finding ψ_0 at the peak of the main beam, and a suitable starting value here is any point just slightly less than π, e.g. 3.

In the formation of the Jacobian matrix A one needs the partial derivatives of $G(\psi, x)$ with respect to the components of x. These are

$$\frac{\partial G}{\partial a_n} = \frac{Me^{a_n}[e^{a_n} - \cos(\psi - b_n)]}{D_n} \qquad (23)$$

$$\frac{\partial G}{\partial b_n} = -\frac{Me^{a_n}\sin(\psi - b_n)}{D_n}$$

$$= -\frac{M\sin(\psi - b_n)}{2(1 - \cos(\psi - b_n))} \quad \text{if } a_n = 0 \qquad (24)$$